NUCL SCI TECH (2020) 31:47
https://doi.org/10.1007/s41365-020-00757-y

Vibrational, rotational, and triaxiality features in extended O(6) dynamical symmetry of IBM using three-body interactions

A. M. Khalaf[1] · Azza O. El-Shal[2] · M. M. Taha[2] · M. A. El-Sayed[2]

Received: 8 December 2019 / Revised: 6 February 2020 / Accepted: 12 February 2020 / Published online: 30 April 2020

Abstract The shape transition between the vibrational U (5) and deformed γ-unstable O(6) dynamical symmetries of sd interacting boson model has been investigated by considering a modified O(6) Hamiltonian, providing that the coefficients of the Casimir operator of O(5) are N-dependent, where N is the total number of bosons. The modified O(6) Hamiltonian does not contain the number operator of the d boson, which is responsible for the vibrational motions. In addition, the deformation features can be achieved without using the SU(3) limit by adding to the O (6) dynamical symmetry the three-body interaction $[QQQ]^{(0)}$, where Q is the O(6) symmetric quadrupole operator. Moreover, triaxiality can be generated through the inclusion of the cubic d-boson interaction $\left[d^{\dagger}d^{\dagger}d^{\dagger}\right]^{(3)}\cdot[\tilde{d}\tilde{d}\tilde{d}]^{(3)}$. The classical limit of the potential energy surface (PES), which represents the expected value of the total Hamiltonian in a coherent state, is studied and examined. The modified O(6) model is applied to the even–even $^{124-132}$Xe isotopes. The parameters for the Hamiltonian and the PESs are calculated using a simulated search program to obtain the minimum root mean square deviation between the calculated and experimental excitation energies and $B(E2)$ values for a number of low-lying levels. A good agreement between the calculations and experiment results is found.

Keywords Nuclear structure · Extended O(6) of IBM · Three-body interactions · Coherent state

1 Introduction

The simplest standard version of the interacting boson model (IBM1) [1] has been widely used for describing the collective nuclear quadrupole states observed in medium and heavy nuclei. The building blocks of this model are pairs of correlated nucleons with angular momentum $L^{\pi} = 0^{+}$ and 2^{+}, which are represented by s and d bosons, respectively. In its simplest version, the model does not distinguish between proton and neutron bosons. According to this algebraic model, the dynamical symmetries are given by U(5) corresponding to spherical vibrator nuclei, SU(3) corresponding to the axially deformed prolate nuclei, and O(6) corresponding to γ-unstable deformed nuclei.

The shape transitions correspond to break these dynamical symmetries. The critical point symmetry E(5) [2] is designed for the critical point of transition from spherical vibrator U(5) to the deformed γ-unstable O(6). Later, X(5) [3] and Y(5) [4] describe the critical points between the spherical vibrator U(5) and axially deformed prolate rotor SU(3), and between SU(3) and the triaxial deformed shapes, respectively. The correspondence between E(5) in IBM and the solution to the Bohr Hamiltonian in the collective model was studied [5–9], and the existence of an additional prolate–oblate transition was recognized [10]. The U(5)–O(6) shape phase transition

✉ M. A. El-Sayed
mathelgohary@yahoo.com

1 Physics Department, Faculty of Science, Al-Azhar University, Cairo, Egypt

2 Mathematics and Theoretical Physics Department, Nuclear Research Center, Atomic Energy Authority, Cairo 13759, Egypt

based on the concepts of the E(5) critical point dynamical symmetry and the quasi-dynamical symmetry was studied [6–11].

Applying the coherent state formalism [12, 13] to an arbitrary Hamiltonian of the three limiting cases of IBM, as well as to a Hamiltonian represented transition within the region among them, the potential energy surface (PES) can be derived by calculating the expected value of this Hamiltonian, which is related to certain nuclear shapes. Because it is known that IBM1, with only up to two-body interactions, cannot give rise to stable triaxial shapes [14, 15], the inclusion of higher-order interactions in the Hamiltonian, such as three-body interactions between d bosons, must be added [16, 17]. In addition, the effects of three-body interactions in an O(6) Hamiltonian have been considered [18–20]. The collective structure of the nuclei in the $A \sim 130$ mass region was discussed within the framework of a rigid triaxial rotor model [21–23] and IBM [1], where the O(6) dynamical symmetry limit was used [19, 24, 25] instead of a geometric γ-unstable rotor model [26]. The even–even xenon nuclei in this mass region $A \sim 130$ are soft with regard to the γ-deformation at an almost maximum effective triaxiality with $\gamma \simeq 30^\circ$ [27, 28].

The triaxiality in Xe, Ba, and Te nuclei within the mass region $A \sim 130$ were studied experimentally [29–33] and interpreted by several nuclear models [34–38]. In this study, we consider the effects of adding terms of cubic d-boson interactions and three $[QQQ]$ interactions (when Q is the O(6) symmetric quadrupole operator) to the symmetry O(6) sdIBM Hamiltonian to generate rotational and triaxial nuclear states. This extended O(6) model with the inclusion of a cubic d-boson interaction, and the inclusion of three-body O(6) symmetric quadrupole terms enables a description of the rotational motion without the use of the SU(3) limit of IBM1 and also allows studying the prolate–oblate shape phase transition. The model is applied to the spectroscopy of the even–even xenon isotopes by calculating the PESs using the intrinsic coherent state formalism.

2 O(6) Hamiltonian of interacting boson model with three-body interactions

The Hamiltonian we used is given by the following weighted sum of three terms:

$$\hat{H} = H_{\mathrm{O(6)}} + H_{3d} + H_Q, \tag{1}$$

where the first term in the Hamiltonian (1) represents the most general O(6) dynamical symmetry Hamiltonian and is written in a multipole form as follows:

$$H_{\mathrm{O(6)}} = a_0(\hat{P}^\dagger \cdot \hat{P}) + a_1(\hat{L} \cdot \hat{L}) + a_3(\hat{T}_3 \cdot \hat{T}_3), \tag{2}$$

where a_0, a_1, a_3 are the model parameters of the Hamiltonian. The operators $\hat{P}, \hat{L}$, and $\hat{T}_3$ are the pairing, angular momentum, and octupole operator, respectively. The explicit expressions for these operators are given as follows:

$$\begin{aligned} \hat{P}^\dagger &= \frac{1}{2}(d^\dagger \cdot d^\dagger - s^\dagger \cdot s^\dagger), \\ \hat{L} &= \sqrt{10}\left[d^\dagger \otimes \tilde{d}\,\right]^{(1)}, \\ \hat{T}_3 &= \left[d^\dagger \otimes \tilde{d}\,\right]^{(3)}. \end{aligned} \tag{3}$$

Here, $s^\dagger$ and $d^\dagger$ are the creation operators of s and d bosons, and $\tilde{d}$ is the annihilation operator of the d boson. The scaler product is defined as $\hat{T}_L \cdot \hat{T}_L = \sum_M (-1)^M T_{LM} T_{L,-M}$, where T_{LM} corresponds to the M-component of the operator $\hat{T}_L$. The operators $\tilde{d}_m = (-1)^m d_{-m}$ and $\tilde{s} = s$ are introduced to ensure the correct tensorial characteristic under spatial rotations.

In general, the one- and two-body sdIBM Hamiltonian give rise to spherical, axially symmetric, and γ-unstable shape deformations. There are no stable triaxially deformed nuclear shapes, unless one includes three-body interactions to break the IBM dynamical symmetries. Thus, to introduce a degree of rotation and triaxiality (γ-dependent), three-body interactions are considered in the second and third terms of Hamiltonian (1).

The second term contains three creation and annihilation operators of the d bosons in a general form as follows:

$$\hat{H}_{3d} = \sum_L \theta_L \left[d^\dagger \otimes d^\dagger \otimes d^\dagger\right]^{(L)} \cdot \left[\tilde{d} \otimes \tilde{d} \otimes \tilde{d}\,\right]^{(L)}, \tag{4}$$

where θ_L is a strength parameter. There are five linear independent combinations of type (4), which are determined uniquely by the value of L $(L = 0, 2, 3, 4, 6)$. We will choose the single third-order interaction between the d bosons (all $\theta_L = 0$ except θ_3), because $L = 3$ is the most effective at creating a triaxial minimum on the potential energy surface. Then, the $L = 3$ cubic d-boson interaction yields the following:

$$\hat{H}_{3d} = \theta_3 \left[d^\dagger \otimes d^\dagger \otimes d^\dagger\right]^{(3)} \cdot \left[\tilde{d} \otimes \tilde{d} \otimes \tilde{d}\,\right]^{(3)}. \tag{5}$$

The third term in Hamiltonian (1) is the cubic quadrupole operator and is written in the following form:

$$\hat{H}_Q = -k[Q \otimes Q \otimes Q]^{(0)} \tag{6}$$

with coupling parameter k, and where $\hat{Q}$ is the O(6) symmetric quadrupole operator of the sdIBM given by

$$\hat{Q} = \left[d^{\dagger}s + s^{\dagger}\tilde{d}\right]^{(2)}. \tag{7}$$

3 Boson intrinsic coherent state

The geometrical interpretation of the IBM Hamiltonian can be obtained by introducing an intrinsic coherent state, which allows associating a geometrical shape to it in terms of the deformation parameter β and a departure from axial symmetry γ ($\beta \geq 0, 0 \leq \gamma \leq \pi/3$).

The intrinsic coherent state of sdIBM for a nucleus with N valence bosons is given by [12]

$$|\ C\ \rangle = \frac{1}{\sqrt{N!}}\left(b_{\mathrm{c}}^{\dagger}\right)^{N}|0\rangle, \tag{8}$$

where $|0\rangle$ represents a boson vacuum (inert core) and $b_{\mathrm{c}}^{\dagger}$ is a boson creation operator given by the following:

$$b_{\mathrm{c}}^{\dagger} = \frac{1}{\sqrt{1+\beta^2}}\left[s^{\dagger} + \beta\cos\gamma d_0^{\dagger} + \frac{1}{\sqrt{2}}\sin\gamma(d_2^{\dagger} + d_{-2}^{\dagger})\right]. \tag{9}$$

In terms of the parameters β and γ, the expected value of the Hamiltonian is easily obtained from the evaluation of the expected values of each single term.

4 Potential energy surface (PES) and critical points

The PES associated with the classical limit of the Hamiltonian $H_{\mathrm{O(6)}}$ is given by its expected value in an intrinsic coherent state (8), yielding the following energy function:

$$\begin{aligned} E_{\mathrm{O(6)}}(N,\beta) &= \left\langle C|H_{\mathrm{O(6)}}|C\right\rangle \\ &= \frac{1}{4}a_0N(N-1)\left(\frac{1-\beta^2}{1+\beta^2}\right)^2 + 6a_1N\frac{\beta^2}{1+\beta^2} \\ &\quad + \frac{7}{5}a_3N\frac{\beta^2}{1+\beta^2}. \end{aligned} \tag{10}$$

Equation (10) can be rewritten in another form:

$$E_{\mathrm{O(6)}}(N,\beta) = \frac{A_2\beta^2 + A_4\beta^4}{(1+\beta^2)^2} + c, \tag{11}$$

where the coefficients A_2, A_4, c are given by

$$\begin{aligned} A_2 &= \lambda N - a_0N(N-1), \\ A_4 &= \lambda N, \\ c &= \frac{1}{4}a_0N(N-1), \end{aligned} \tag{12}$$

with $\lambda = 6a_1 + \frac{7}{5}a_3$.

The PES Eq. (11) is γ-independent and has two independent parameters a_0 and λ.

To analyze the critical behavior for the energy function Eq. (11), the anti-spinodal point occurs when E becomes flat at $\beta = 0$ or when $\partial^2E/\partial\beta^2|_{\beta=0} = 0$ ($A_2 = 0$), which yields $\frac{a_0(N-1)}{\lambda} = 1$.

The deformed nucleus has the absolute minimum at $\beta \neq 0$. For any stable equilibrium state, the first derivative of E with respect to β must be zero, and the second derivative must be positive. Thus, we obtain the following:

$$A_2 + (2A_4 - A_2)\beta^2 = 0, \tag{13}$$

$$A_2 + (6A_4 - 8A_2)\beta^2 - (6A_4 - 3A_2)\beta^4 > 0. \tag{14}$$

Therefore, the equilibrium value of β is as follows:

$$\beta_0 = \pm\sqrt{\frac{A_2}{A_2 - 2A_4}} = \pm\sqrt{\frac{a_0(N-1) - \lambda}{a_0(N-1) + \lambda}}. \tag{15}$$

Under the condition $a_0(N-1) > \lambda$, the critical point is found at $\lambda = a_0(N-1)$, and the corresponding E becomes the following:

$$E_{\mathrm{critical}} = \frac{\lambda N\beta^4}{(1+\beta^2)^2} + \frac{1}{4}a_0N(N-1). \tag{16}$$

In Table 1 and Fig. 1, we show the PES calculations corresponding to the modified O(6) limit for different values of N ($N = 2, 4, 7, 10, 12$). In Fig. 1, we show that the critical point of a shape transition depends on the total number of bosons N. We adjusted the PES parameters listed in Table 1 to produce a shape transition at the critical $N = 7$, which for the value $N = 7$ gives a flat β^4 surface at $\beta = 0$. Five values of N are presented, one at the critical value of $N = 7$, and two below and two above this value. For $N < 7$, the nucleus is in a symmetric phase because the PES has a unique minimum at $\beta = 0$, meaning a spherical shape under equilibrium is obtained. When N increases to the critical point $N = 7$, the non-symmetric and symmetric minima attain the same depth, whereas for $N > 7$ the shape at equilibrium is deformed.

In a classical limit ($N \to \infty$), the PES is not explicitly dependent on N and is given by the following:

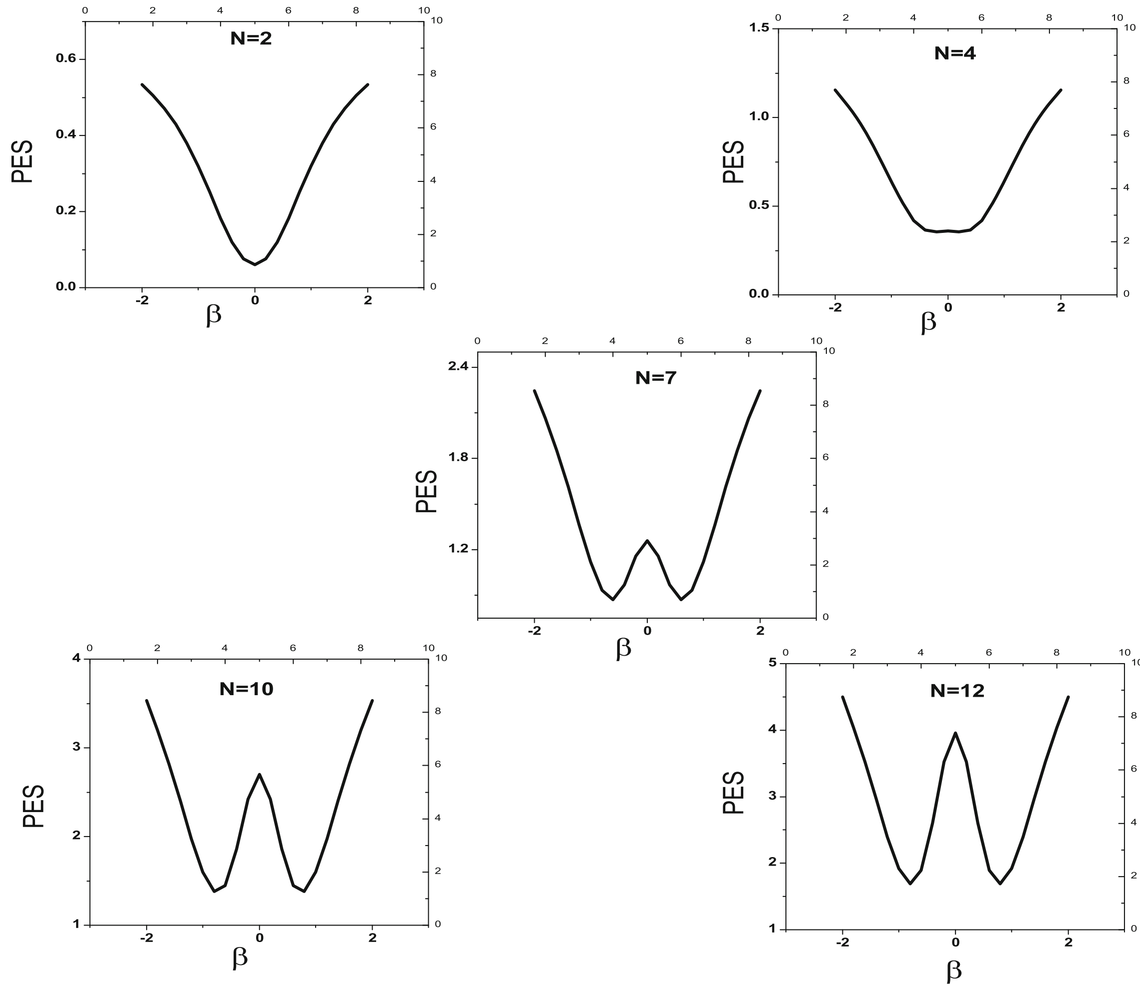

Fig. 1 PESs versus the deformation parameter β for the data listed in Table 1

Table 1 Parameters of the PES for a set of boson numbers $N = 2, 4, 7, 10, 12$ (a_0 = 0.12 MeV, λ = 0.320 MeV)

N	2	4	7	10	12
A_2	0.4	− 0.16	− 2.8	− 7.6	− 12
A_4	0.64	1.28	2.24	3.2	3.84
c	0.06	0.36	1.26	2.70	3.96

$$E(\beta) = \frac{(\lambda - a_0)\beta^2 + \lambda\beta^4}{(1+\beta^2)^2} + \frac{1}{4}a_0. \tag{17}$$

Introducing the parameter x such that $x = a_0/\lambda$, Eq. (17) can be written as follows:

$$\frac{E(\beta)}{\lambda} = \frac{(1-x)\beta^2 + \beta^4}{(1+\beta^2)^2} + \frac{1}{4}x \tag{18}$$

For $x < 1$, the global minimum is at $\beta = 0$. For $x > 1$, we arrive at a deformed γ-soft shape. For $x = 1$, a second-order phase transition from a spherical to deformed shape occurs (flat β^4 surface).

Figure 2 shows the evolution of the PESs for various values of x, where a shape phase transition occurs at $x = 1$, providing a flat β^4 surface close to $\beta = 0$; that is, the classical limit has the capability of producing a shape transition.

An N dependence occurs if we modify the O(6) Hamiltonian of the sd IBM Eq. (2) by providing the coefficients a_1, a_3 of the Casimir operator of O(5) ($C_2[\mathrm{O}(5)] \sim a_1 L \cdot L + a_3 T_3 \cdot T_3$), which are N dependent, that is, $a_1 = f_1 + g_1 N, a_3 = f_3 + g_3 N$, and the modified O(6) Hamiltonian in this case becomes the following:

$$H^{\text{modified}}_{\mathrm{O}(6)} = a_0 P^{\dagger} P + (f_1 + h_1 N) L \cdot L + (f_3 + h_3 N) T_3 \cdot T_3. \tag{19}$$

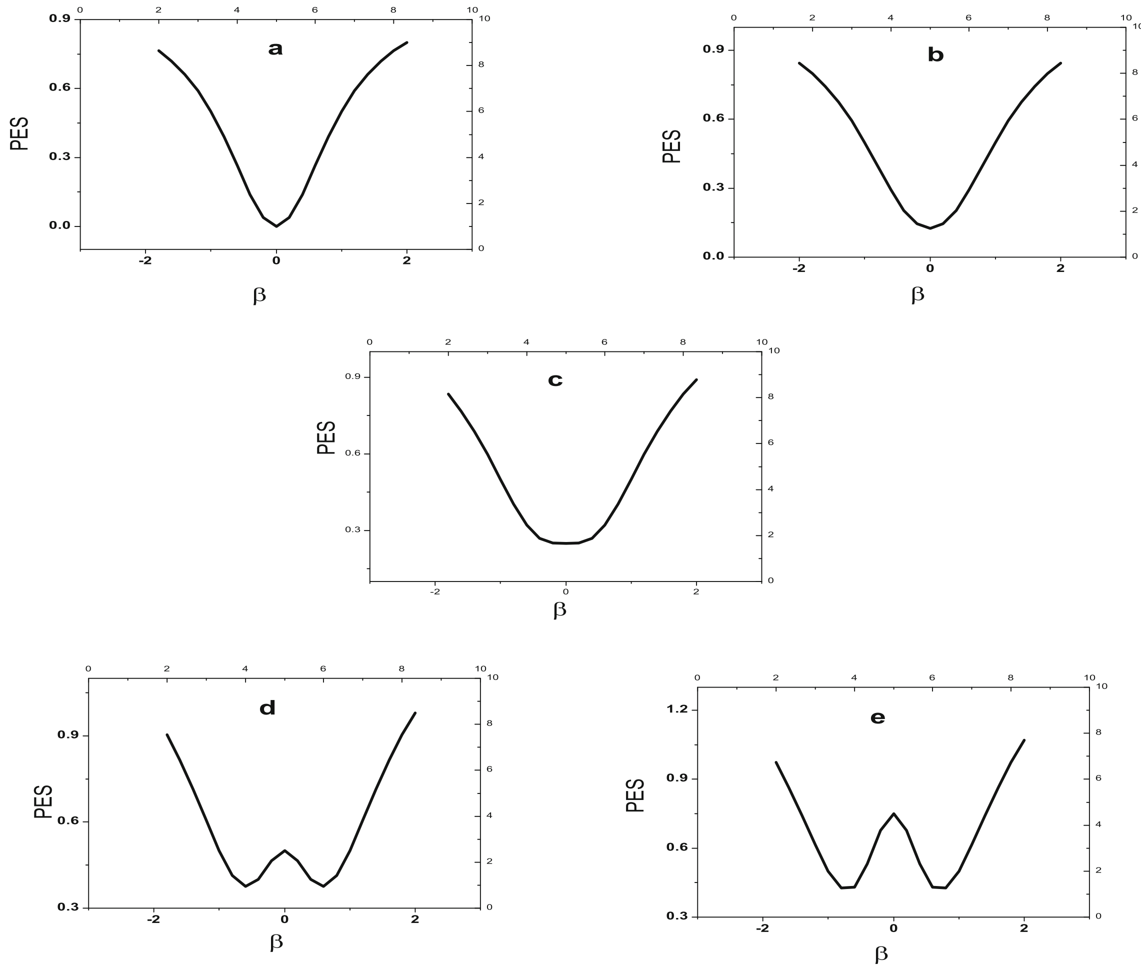

Fig. 2 PESs of the O(6) dynamical symmetry of IBM at the classical limit as a function of the deformation parameter β for **a**, **b** a spherical shape ($x = 0$, $x = 0.5$), **c** a flat β^4 surface ($x = 1$), and **d**, **e** a deformed shape ($x = 2$, $x = 3$)

This Hamiltonian is not U(5) invariant but exhibits properties of a spherical vibrator to a high degree of accuracy despite not containing a $\hat{n}_d$ operator. The PES for this modified O(6) Hamiltonian is also given by Eq. (11) with $\lambda = \left(6f_1 + \frac{7}{5}f_3\right) + N\left(6h_1 + \frac{7}{5}h_3\right)$.

Equation (11) can be written in the following form:

$$E(N,\beta) = \frac{g_2\beta^2 + g_4\beta^4 + g_6\beta^6}{(1+\beta^2)^3} + c, \tag{20}$$

where

$$\begin{aligned} g_2 &= A_2 = \lambda N - a_0 N(N-1),\\ g_4 &= A_2 + A_4 = 2\lambda N - a_0 N(N-1),\\ g_6 &= A_4 = \lambda N. \end{aligned} \tag{21}$$

The expected value of the cubic d-boson Hamiltonian H_{3d} is obtained using the intrinsic coherent state (8), yielding the following:

$$\begin{aligned} E_{3d}(N,\beta,\gamma) &= \frac{1}{7}\theta_3 N(N-1)(N-2)\frac{\beta^6}{(1+\beta^2)^3}\\ &\quad\times(-1+\cos^2 3\gamma)\\ &= \frac{a\beta^6\cos^2 3\gamma - a\beta^6}{(1+\beta^2)^3}, \end{aligned} \tag{22}$$

where

$$a = \frac{1}{7}\theta_3 N(N-1)(N-2). \tag{23}$$

In addition, the classical potential corresponding to the three-body Hamiltonian H_Q using the intrinsic coherent state (8) is given by the following:

$$E_Q(N,\beta,\gamma) = -K\sqrt{\frac{8}{35}}\left[\frac{3N(N-1)}{(1+\beta^2)^3} + \frac{4N(N-1)(N-2)}{(1+\beta^2)^3}\right] \times \beta^3\cos 3\gamma = \frac{g_3\beta^3\cos 3\gamma + g_5\beta^5\cos 3\gamma}{(1+\beta^2)^3}, \tag{24}$$

where

$$g_3 = -K\sqrt{\frac{8}{35}}N(N-1)(4N-5), \quad g_5 = -3K\sqrt{\frac{8}{35}}N(N-1). \tag{25}$$

Adding Eqs. (22) and (24) corresponding to the three-body interactions to Eq. (11), which describes the O(6) dynamical symmetry, yields the total PES of the total Hamiltonian (1).

$$E(N,\beta,\gamma) = \frac{1}{(1+\beta^2)^3}\left[g_2\beta^2 + g_3\beta^3\cos 3\gamma + g_4\beta^4 + g_5\beta^5\cos 3\gamma + (g_6-a)\beta^6 + a\beta^6\cos^2 3\gamma + g_0\right]. \tag{26}$$

This final formula for the PES contains seven parameters, $\{g_2, g_3, g_4, g_5, g_6, a, g_0\}$, in addition to the γ angle.

5 B(E2) ratios

Calculations of the excitation energies and electric quadrupole reduced transition probabilities $B(E2)$ provide a good test for shaping the transition. The electric quadrupole transition operator in the O(6) limit of IBM is given by the following [39]:

$$\hat{T}(E2) = e\left[d^\dagger \times \tilde{s} + s^\dagger \times \tilde{d}\right]^{(2)} \tag{27}$$

with e being the boson effective charge. The reduced electric quadrupole transition probabilities are given by the following:

$$B(E2; I_i \to I_f) = \frac{1}{2I_i+1}\left|\langle I_f || \hat{T}(E2) || I_i\rangle\right|^2, \tag{28}$$

where I_i and I_f are the angular momenta for the initial and final states, respectively. For the ground state band, the energy ratios $R_{I/2}$ and the ratios of the $E2$ transition rates $B_{I+2/2}$ are defined as follows:

$$R_{I/2} = \frac{E(I_i^+)}{E(2_1^+)}, \quad B_{I+2/2} = \frac{B(E2; I+2 \to I)}{B(E2; 2_1^+ \to 0_1^+)}. \tag{29}$$

The ratios for the U(5) and O(6) limits of IBM are given by the following:

$$R_{I/2} = \left\{\begin{array}{ll} \frac{I}{2} & \text{for U(5)} \\ \frac{I}{8}\left(\frac{I}{2}+3\right) & \text{for O(6)} \end{array}\right\}, \tag{30}$$

$$B_{I+2/2} = \left\{\begin{array}{ll} \frac{1}{2}(I+2)\left(1-\frac{I}{2N}\right) & \text{for U(5)} \\ \frac{5}{2}\frac{(I+2)}{(I+5)}\left(1-\frac{I}{2N}\right)\left(1+\frac{I}{2(N+4)}\right) & \text{for O(6)} \end{array}\right\}. \tag{31}$$

6 Numerical calculations and discussion

To visualize the influence of the cubic boson interaction term on the PES plots, we first represent the PES for the pure O(6) limit Eq. (11) with parameters $A_2 = -2.96, A_4 = 2.64, c = 1.4$ (all in MeV), as shown in Fig. 3a. It is known that the shape of the general one- and two-body IBM1 Hamiltonian at equilibrium can never be triaxial. Only the inclusion of specific higher-order boson interaction terms [at least three-body interactions such as H_{3d} in Eq. (5) and H_Q in Eq. (6)] produces triaxiality. The influence of the cubic term H_{3d} of the O(6) limit is studied by plotting the PESs in Fig. 3b–d according to $H_{O(6)} + H_{3d}$ with the parameters $g_2 = -2.96, g_4 = -0.32, g_6 = 2.64, a = 2.88, c = 1.4$ (all in MeV). It can be seen that a stable triaxial minimum results at $\gamma = 30^\circ$ and $\beta = 0.7$.

When the strength parameter of the cubic term H_{3d} equals zero (a = 0), a minimum in PES with respect to γ can only occur for $\gamma = 0^\circ$ or $\gamma = 60^\circ$; that is, the equilibrium shape of the classical limit can never be triaxial. For $a \neq 0$, the cubic term lowers the PES with the greatest effect occurring at $\beta_0 \neq 0$ and $\gamma = 30^\circ$. Figure 4 illustrates the PESs of $E_{O(6)} + E_{3d}$ according to Eqs. (11) and (22) in the classical limit.

For the three-body O(6) symmetric quadrupole term H_Q, for a fixed λ in Eq. (11) and $k \neq 0$ in Eq. (24), the surface energy depends on γ and leads to triaxiality. Figure 5 shows the calculated PESs for $k \neq 0$ and various values of the coefficient of the pairing operator a_0.

- For $a_0 = 0$, the minimum potential surface occurs at $k > 0$, $\gamma = 0$, or $k < 0$, where $\gamma = 0^\circ$ and the PES exhibit spherical ($\beta = 0$) and deformed ($\beta > 0$) shapes (panel a)
- For $a \neq 0$, a spherical shape occurs for $a_0 < \lambda$ (panel b) and a deformed shape occurs for $a_0 > \lambda$ (panels d and e).
- For $a_0 = \lambda$, the spherical shape disappears (panel c)

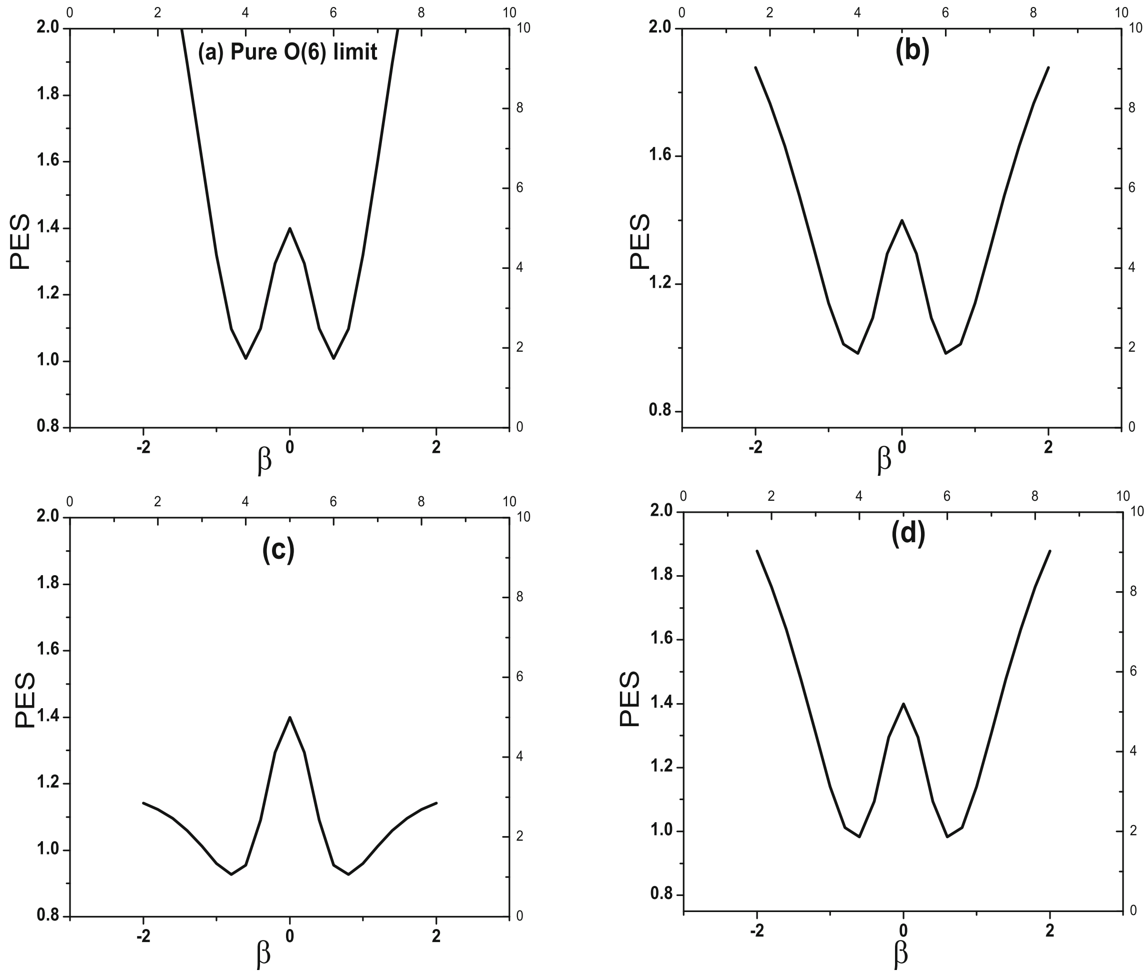

Fig. 3 PES as a function of β

The even–even transitional nuclides $^{124-132}$Xe represent an excellent example for the extended O(6) triaxial shapes. Because the neutron numbers in this isotopic chain are between $N = 70$ and $N = 78$, the doubly closed shell of $Z = 50$ and $N = 82$ is assumed such that the neutrons are treated as holes, whereas the protons are valance particles when we determine the total number of bosons. For each nucleus, the parameters of the PESs $g_2, g_3, g_4, g_5, g_6, a, g_0, \gamma$, which depend on the original parameters of our proposed Hamiltonian, are adjusted from a best fit to the experimental data of the level energies, $B(E2)$, which are the transition probabilities for the ground state bands. A standard χ test is used to conduct the fitting

$$\chi = \sqrt{\frac{1}{n}\sum_{i=1}^{N}\left[\frac{X_i(\text{data}) - X_i(\text{IBM})}{\delta X_i(\text{data})}\right]^2}, \tag{32}$$

where n is the number of experimental data points; $X_i(\text{data})$ and $X_i(\text{IBM})$ are the experimental and calculated spectroscopic properties, respectively; and $\delta X_i(\text{data})$ indicates experimental errors. The experimental data include six energies of levels $2_1, 2_2, 4_1, 3_1, 4_2, 8_1$, and five $B(E2)$ reduced quadrupole transition probabilities of the transition $2_1^+ \to 0_1^+, 4_1^+ \to 2_1^+, 2_2^+ \to 2_1^+, 2_2^+ \to 0_1^+, 2_1^+ \to 0_2^+$, and low-spin ground states. The best adopted parameters are listed in Table 2. A comparison between the experimental and our extended O(6)$_{\text{IBM}}$ calculations for the energy ratios $R_{I_i^+/2_1^+} = E(I_i^+)/E(2_1^+)$ and $B(E2)$ ratios $B_{I+2/2}$ is shown in Tables 3 and 4. For the pure O(6), the ratios are $R_{2_2^+/2_1^+} = 2.235$, $R_{4_1^+/2_1^+} = 2.647$, $R_{3_1^+/2_1^+} = 4.058$, $R_{4_2^+/2_1^+} = 4.294$, and $R_{6_1^+/2_1^+} = 4.941$.

A good agreement between the present calculations and the experiment results was found. We can see that the collectivity increases smoothly with a decrease in the neutron number from $N = 78$ to $N = 70$, and the value of the $R_{4/2}$ ratio changes from the vibrational limit $R_{4/2} \simeq 2$ for ^{132}Xe to γ-soft rotor $R_{4/2} \simeq 2.5$ for ^{124}Xe.

In Table 4 and Fig. 6, we give the values of the calculated ratios of the $E2$ transition rates $B_{I+2/2}$ for ^{124,128,132}Xe compared to the experimental values and to the calculated O(6) prediction.

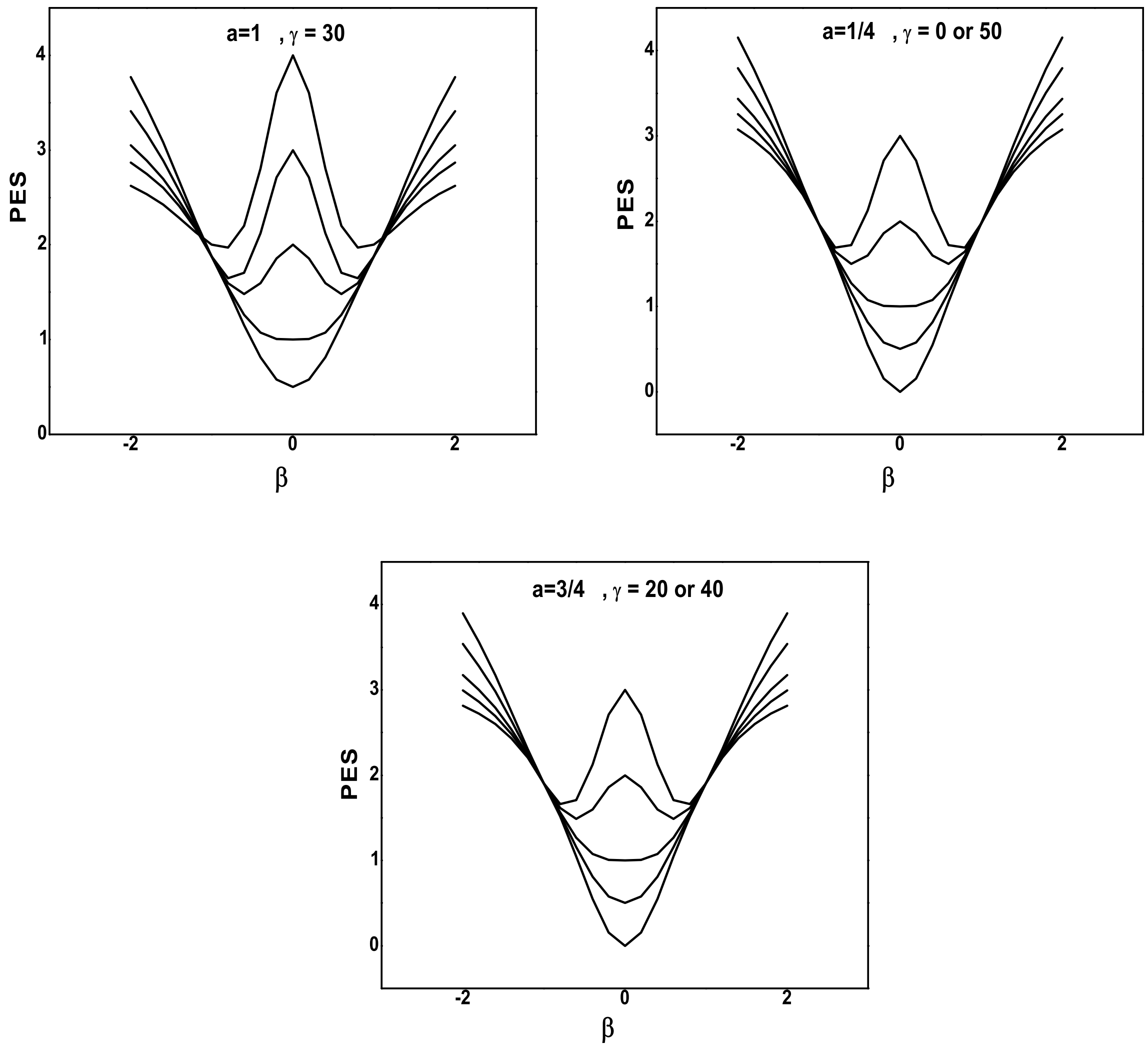

Fig. 4 PESs according to $H_{O(6)} + H_{3d}$ in the classical limit as a function of deformation parameters β, demonstrating the influence of the departure from the axial symmetry γ and the strength parameter a of the cubic terms with three creation and three annihilation operators of the d bosons. The parameter a_0 is indicated in the figure, and $\lambda = 4$

The results of the extended $O(6)_{IBM}$ triaxial calculations for the classical limit of the evolution of the PESs for the even–even $^{124-132}$Xe isotopic chain are shown in Fig. 7 as a function of the deformation parameter β_2, the PES parameters of which are listed in Table 2. From Table 2, we can see that for ^{132}Xe the parameters g_3 and g_5 have positive values compared to those of the otherXe isotopes because ^{132}Xe shows a quasi-vibrational nucleus demonstrating a minimum PES in the form of a narrow (β, γ) valley from the spherical region $(k<0)$ to the triaxial region $(k>0)$ with $\gamma \simeq 30^\circ$ (where k is the strength parameter of the three-body O(6) symmetric quadrupole term). On the other side, the isotope ^{124}Xe is a candidate for a deformed O(6) triaxial in a ground state with the shallow minima at $\gamma \simeq 26^\circ$. The resulting contour PESs for ^{124}Xe and ^{126}Xe are shown in Fig. 8.

7 Conclusion

The effects of three-body boson interactions were considered. Three d-boson interactions $\left[d^\dagger d^\dagger d^\dagger\right]^{(3)} \cdot \left[\tilde{d}\tilde{d}\tilde{d}\right]^{(3)}$ and the cubic $[QQQ]^{(0)}$ terms, where Q is the O(6) symmetric quadrupole operator, are added to the Hamiltonian of the extended O(6) dynamical symmetry of the IBM. We provided the coefficients of the Casimir operator of O(5), which are N-dependent, where N is the total number of bosons. The modified O(6) model exhibits rotational and triaxiality behaviors. The model is applied to the even–even $^{124-132}$Xe isotopes. A simulated fitting procedure is conducted to obtain the model parameters for each nucleus of the Xe isotopic chain and thus the minimum root mean square deviation between the calculated and

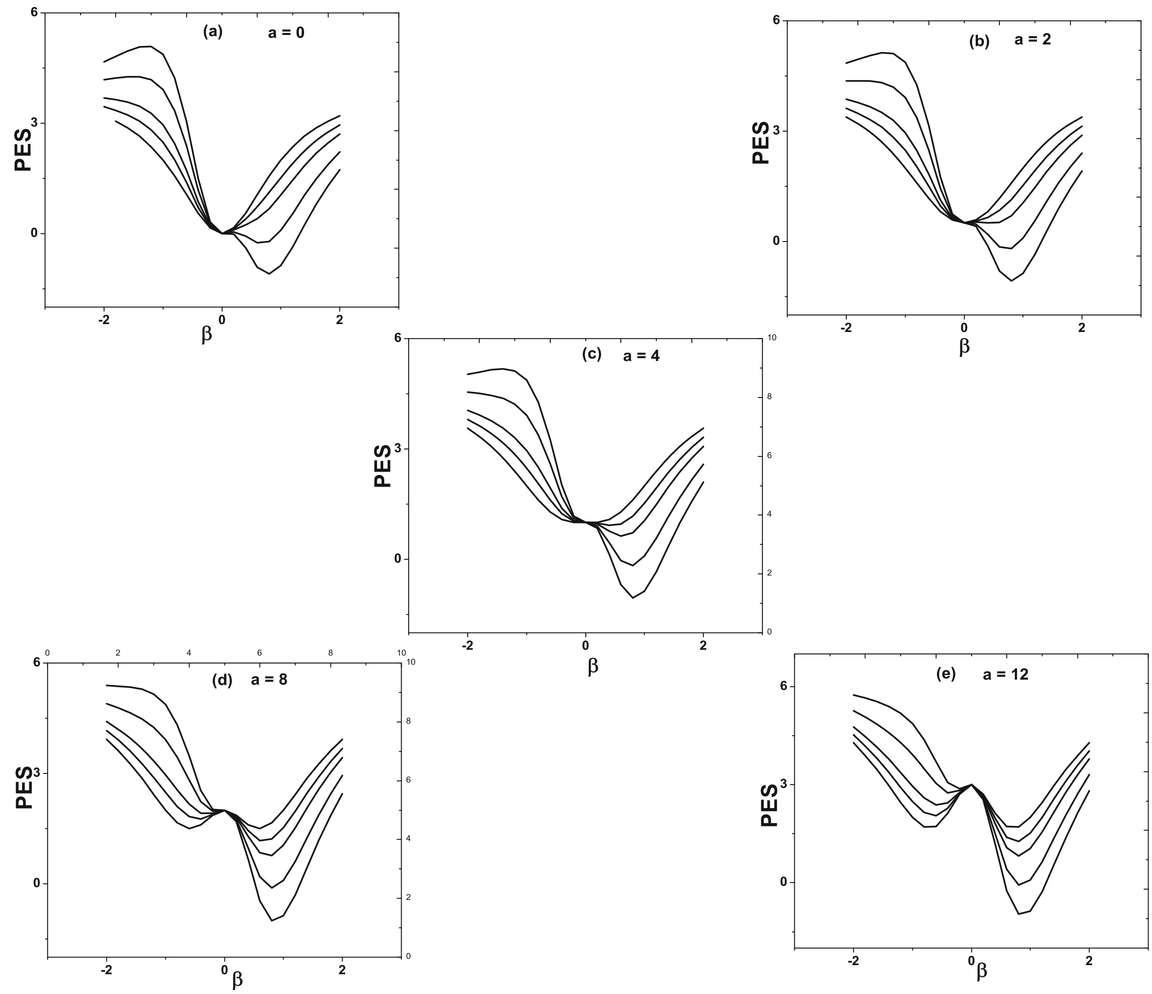

Fig. 5 PES Equations (11) and (24) in the classical limit as a function of deformation parameter β showing the influence of the strength parameter k of the cubic term interaction $[QQQ]^{(0)}$ to introduce a degree of triaxiality. The parameter a_0 is indicated in the figure, and $\lambda = 4$

Table 2 Values of the adopted best PES parameters (in MeV) as derived through the fitting procedure used in the present calculations for a $^{124-132}$Xe isotopic chain (where N is the boson number)

	^{124}Xe $N = 8$	^{126}Xe $N = 7$	^{128}Xe $N = 6$	^{130}Xe $N = 5$	^{132}Xe $N = 4$
g_2	1.24	1.26	1.23	1.15	1.05
g_4	3.88	3.57	3.21	2.8	2.001
g_6	4.04	3.36	2.73	2.15	2.101
g_3	− 0.158	− 0.118	− 0.084	− 0.056	0.169
g_5	− 0.632	− 0.472	− 0.336	− 0.224	0.076
a	2.88	1.8	1.028	0.514	0.205
g_0	1.4	1.05	0.75	0.5	0.22

Table 3 A comparison between experimental and calculated energy ratios $R_{I_i^+/2_i^+} = E(I_i^+)/E(2_1^+)$ for $^{124-132}$Xe isotopic chain

NB	Nuclide	$R_{2_2^+/2_1^+}$	$R_{4_1^+/2_1^+}$	$R_{3_1^+/2_1^+}$	$R_{4_2^+/2_1^+}$	$R_{6_1^+/2_1^+}$
8	^{124}Xe					
	Cal.	2.376	2.471	3.501	4.100	4.316
	Exp.	2.391	2.482	3.524	4.061	4.373
7	^{126}Xe					
	Cal.	2.211	2.389	3.398	3.893	4.184
	Exp.	2.264	2.423	3.390	3.829	4.207
6	^{128}Xe					
	Cal.	2.141	2.336	3.252	3.699	3.912
	Exp.	2.188	2.332	3.227	3.620	3.922
5	^{130}Xe					
	Cal.	2.045	2.311	3.062	3.365	3.651
	Exp.	2.093	2.247	3.045	3.373	3.626
4	^{132}Xe					
	Cal.	1.911	2.126	2.753	2.912	3.223
	Exp.	1.943	2.157	2.701	2.939	3.162

Table 4 Calculated ratios of $E2$ transition probabilities $B_{I+2/2} = \frac{B(E2;I+2\to I)}{B(E2;2_1^+\to 0_1^+)}$, $I^\pi = 2_1^+$ to 8_1^+ for ^{124,128,132}Xe isotopes compared to those obtained from the experimental results as well as the prediction of the O(6) limit of IBM

NB	Nuclide	$B_{4/2}$	$B_{6/4}$	$B_{8/6}$	$B_{10/8}$
8	^{124}Xe				
	Exp.	1.34(24)	1.59(71)	0.63(29)	0.29(8)
	Cal.	1.501	1.991	2.490	3.354
	O(6)	1.354	1.458	1.420	1.282
6	^{128}Xe				
	Exp.	1.47(2)	1.94(26)	2.39(4)	2.74(114)
	Cal.	1.790	2.853	4.232	6.001
	O(6)	1.309	1.333	1.181	0.897
4	^{132}Xe				
	Exp.	1.24(18)			
	Cal.	2.990	2.032	17.492	
	O(6)	1.205	1.666	0.625	

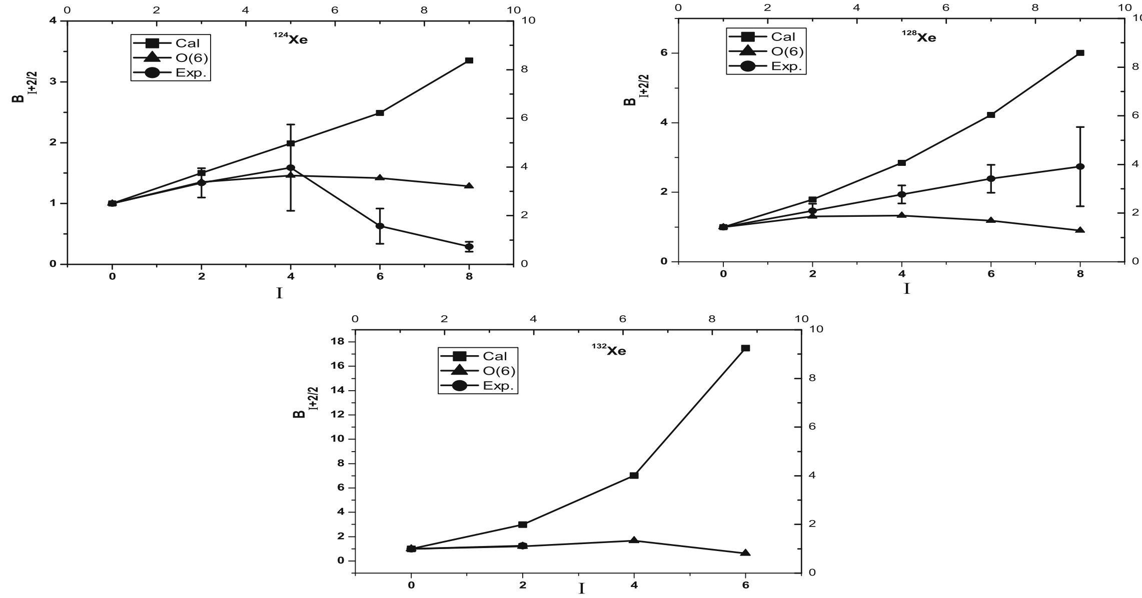

Fig. 6 Comparison of the calculated $B_{I+2/2} = \frac{B(E2;I+2 \to I)}{B(E2;2_1^+ \to 0_1^+)}$ ratios of the ground bands in ^{124}Xe ($NB = 8$), ^{128}Xe ($NB = 6$), and ^{132}Xe ($NB = 4$) compared to the experimental results and O(6) IBM prediction

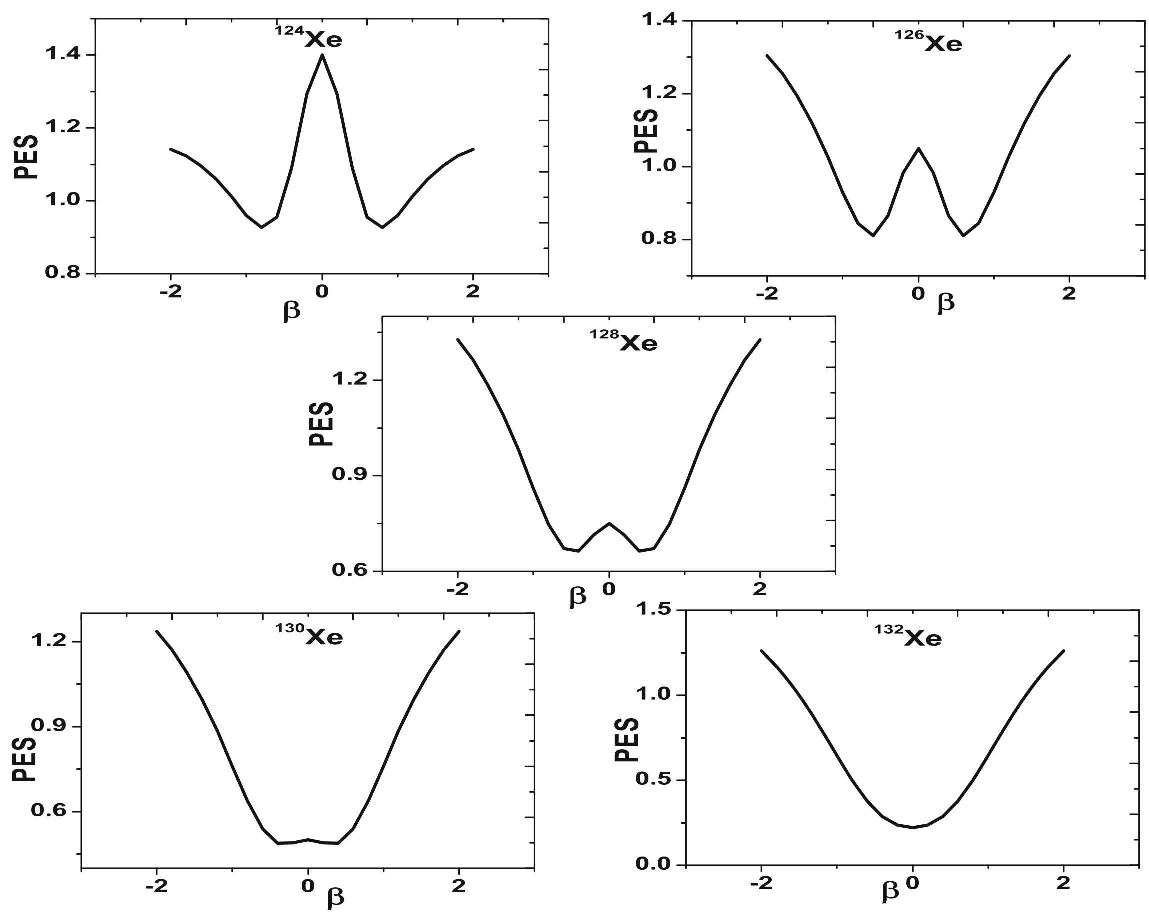

Fig. 7 PES as a function of β for a $^{124-132}$Xe chain

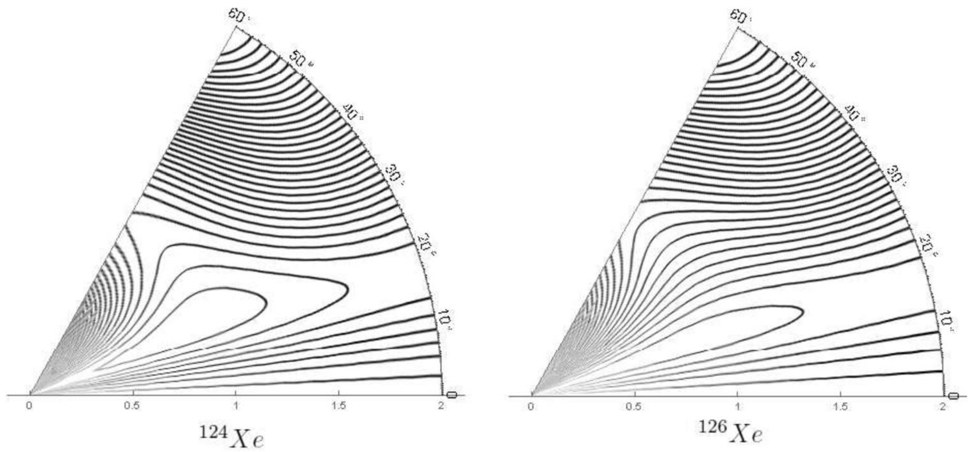

Fig. 8 Contour plots of PESs for the nuclei of ^{124}Xe and ^{126}Xe

experimentally selected set of energy levels and $B(E2)$ transition rates of the yrast states.

References

1. F. Iachello, A. Arima, *The Interacting Boson Model* (Cambridge University Press, Cambridge, 1987). https://doi.org/10.1017/CBO9780511895517
2. F. Iachelko, Dynamic symmetries at the critical point. Phys. Rev. Lett. **85**, 3580 (2000). https://doi.org/10.1103/PhysRevLett.85.3580
3. F. Iachelko, Analytic description of critical point nuclei in a spherical-axially deformed shape phase transition. Phys. Rev. Lett. **87**, 052502 (2001). https://doi.org/10.1103/PhysRevLett.87.052502
4. F. Iachelko, Phase transitions in angle variables. Phys. Rev. Lett. **91**, 132502 (2003). https://doi.org/10.1103/PhysRevLett.91.132502
5. A. Frank, C.E. Alonso, J.M. Arias, Search for E(5) symmetry in nuclei: the Ru isotopes. Phys. Rev. C **65**, 014301 (2002). https://doi.org/10.1103/PhysRevC.65.014301
6. J.E. Arias, C.E. Alonso, A. Vitturi et al., U(5)–O(6) transition in the interacting boson model and the E(5) critical point symmetry. Phys. Rev. C **68**, 041302(R) (2003). https://doi.org/10.1103/PhysRevC.68.041302
7. J.E. Garcia-Ramos, Phase transitions and critical points in the rare-earth region. Phys. Rev. C **68**, 024307 (2003). https://doi.org/10.1103/PhysRevC.68.024307
8. A. Leviaten, J.M. Ginocchio, Critical-point symmetry in a finite system. Phys. Rev. Lett. **90**, 212501 (2003). https://doi.org/10.1103/PhysRevLett.90.212501
9. J.E. Garcia-Ramos, J. Dukelesky, J.M. Arias, β^4 potential at the U(5)–O(6) critical point of the interacting boson model. Phys. Rev. C **72**, 037301 (2005). https://doi.org/10.1103/PhysRevC.72.037301
10. J. Jolie, A. Linnemann, Prolate-oblate phase transition in the Hf–Hg mass region. Phys. Rev. C **68**, 031301(R) (2003). https://doi.org/10.1103/PhysRevC.68.031301
11. D.J. Rowe, Quasidynamical symmetry in an interacting boson model phase transition. Phys. Rev. Lett. **93**, 122502 (2004). https://doi.org/10.1103/PhysRevLett.93.122502
12. J.N. Ginocchio, M.W. Kirson, An intrinsic state for the interacting boson model and its relationship to the Bohr–Mottelson model. Nucl. Phys. A **350**, 31 (1980). https://doi.org/10.1016/0375-9474(80)90387-5
13. A.E.L. Dieperink, O. Scholten, F. Iachello, Classical limit of the interacting-boson model. Phys. Rev. Lett. **44**, 1747 (1980). https://doi.org/10.1103/PhysRevLett.44.1747
14. P. Van Isacker, J.Q. Chen, Classical limit of the interacting boson Hamiltonian. Phys. Rev. C **24**, 684 (1981). https://doi.org/10.1103/PhysRevC.24.684
15. K. Heyde, P. Van Isacker, M. Waroquier et al., Triaxial shapes in the interacting boson model. Phys. Rev. C **29**, 1420 (1984). https://doi.org/10.1103/PhysRevC.29.1420
16. J. E. García-Ramos, C. E. Alonso, J. M. Arias et al., Anharmonic double-γ vibrations in nuclei and their description in the interacting boson model. Phys. Rev. C **61**, 047305 (2000). https://doi.org/10.1103/PhysRevC.61.047305
17. J. E. García-Ramos, J. M. Arias, P. Van Isacker et al., Anharmonic double-phonon excitations in the interacting boson model. Phys. Rev. **C62**, 064309 (2000). https://doi.org/10.1103/PhysRevC.62.064309
18. V. Werner, N. Pietralla, P. von Brentano et al., Quadrupole shape invariants in the interacting boson model. Phys. Rev. C **61**, 021301 (2000). https://doi.org/10.1103/PhysRevC.61.021301
19. P. Van Isacker, Dynamical symmetry and higher-order interactions. Phys. Rev. Lett. **83**, 4269 (1999). https://doi.org/10.1103/PhysRevLett.83.4269
20. G. Thiamova, P. Cejnar, Prolate-oblate shape-phase transition in the O(6) description of nuclear rotation. Nucl. Phys. A **765**, 97–111 (2006). https://doi.org/10.1016/j.nuclphysa.2005.11.006
21. A. Bohr, B.R. Mottelson, *Nuclear Structure*, vol. 2 (Benjamin, Reading, 1975)
22. A.S. Davydov, G.F. Filippov, Rotational states in even atomic nuclei. Nucl. Phys. **8**, 23 (1958). https://doi.org/10.1016/0029-5582(58)90153-6
23. R.F. Casten, *Nuclear Structure from a Simple Prespective* (Oxford University Press, Oxford, 1990)
24. D.J. Rowe, G. Thiamova, The many relationships between the IBM and the Bohr model. Nucl. Phys. A **760**, 59 (2005). https://doi.org/10.1016/j.nuclphysa.2005.06.001
25. G. Thiamova, D.J. Rowe, Large boson number IBM calculations and their relationship to the Bohr model. Eur. Phys. J. A **41**, 189 (2009). https://doi.org/10.1140/epja/i2009-10810-x
26. L. Wilets, M. Jean, Surface oscillations in even–even nuclei. Phys. Rev. **102**, 788 (1956). https://doi.org/10.1103/PhysRev.102.788
27. J. Yan, O. Vogel, P. von Brentano et al., Systematics of triaxial deformation in Xe, Ba, and Ce nuclei. Phys. Rev. C **48**, 1046 (1993). https://doi.org/10.1103/PhysRevC.48.1046

28. O. Vogel, P. Van Isacker, A. Gelberg et al., Effective γ deformation near A = 130 in the interacting boson model. Phys. Rev. C **53**, 1660 (1996). https://doi.org/10.1103/PhysRevC.53.1660
29. R. Kühn, K. Kirch, I. Wiedenhöver et al., Non-yrast states in ^{132}Ba. Nucl. Phys. A **597**, 85-105 (1996). https://doi.org/10.1016/0375-9474(95)00415-7
30. Y.A. Luo, J.Q. Chen, J.P. Draayer, Nucleon-pair shell model calculations of the even–even Xe and Ba nuclei. Nucl. Phys. A **669**, 101 (2000). https://doi.org/10.1016/S0375-9474(99),00818-0
31. B. Saha, A. Dewald, O. Möller et al., Probing nuclear structure of ^{124}Xe. Phys. Rev. C **70**, 034313 (2004). https://doi.org/10.1103/PhysRevC.70.034313
32. C.J. Barton, M.A. Caprio, D. Shapira et al., B(E2) values from low-energy Coulomb excitation at an ISOL facility: the N = 80, 82 Te isotopes. Phys. Lett. B **551**, 269-276 (2003). https://doi.org/10.1016/S0370-2693(02)03066-6
33. N. Turkan, Search for E(5) behavior: IBM and Bohr–Mottelson model with Davidson potential calculations of some even–even Xe isotopes. J. Phys. G Nucl. Part. Phys. **34**, 2235 (2007). https://doi.org/10.1088/0954-3899/34/11/001
34. P. F. Mantica, Jr., B. E. Zimmerman, W. B. Walters et al., Level structure of ^{126}Xe: population of low-spin levels in the decay of 1^{+126}Cs and theoretical description of adjacent even–even Xe nuclides. Phys. Rev. C **45**, 1586 (1992). https://doi.org/10.1103/PhysRevC.45.1586
35. U. Meyer, A. Faessler, S.B. Khadkikar, The triaxial rotation vibration model in the Xe–Ba region. Nucl. Phys. A **624**, 391 (1997). https://doi.org/10.1016/S0375-9474(97)00380-1
36. L. Próchniak, K. Zając, K. Pomorski et al., Collective quadrupole excitations in the 50 $<$ Z, N $<$ 82 nuclei with the general Bohr Hamiltonian. Nucl. Phys. A **648**, 181-202(1999). https://doi.org/10.1016/S0375-9474(99)00023-8
37. Rani Devi, S. P. Sarswat, Arun Bharti et al., E2 transition and Q_{J^+} systematics of even mass xenon nuclei. Phys. Rev. C **55**, 2433 (1997). https://doi.org/10.1103/PhysRevC.55.2433
38. L. Fortunato, A. Vitturi, Analytically solvable potentials for γ-unstable nuclei. J. Phys. G Nucl. Part. Phys. **29**, 1341 (2003)
39. R.F. Casten, *Nuclear Structure From a Simple Prespective, Thomson Learning* (Oxford University Press, Oxford, 1990)